Bull. Disas. Prev. Res. Inst., Kyoto Univ., Vol. 32, Part 2, No 289, June, 1982

Earthquake Ground Motions Influenced by Horizontally Discontinuous Structures

By Shigeru KASUGA and Kojiro IRIKURA

(Manuscript received March 31, 1982)

Abstract

We observed earthquake ground motions at the area where the underground structures contain a horizontally irregular interface with abrupt change of sedimentary layer thickness. Amplification effects due to underground structures are estimated from the spectral ratios of S wave ground motions at the soft ground to those at the rock outcrop. The spectral ratios show that amplification effects are influenced by the underground structures including adjacent areas in propagation of seismic waves. Predominant frequencies of the amplifications at the several points near and across the horizontal discontinuity are similar to each other, although the amplification factors at the predominant frequencies increase with the increasing thickness of the soft surface layer. These observed results are not consistent with the theoretical responses calculated by conventional Tomson-Haskell matrix method.

Seismic responses for incident SH waves are calculated in a multilayered medium containing a layer with a horizontal discontinuity (i.e. laterally varying structure), applying the following two methods: singular integral equation method developed by Kennett, and discrete wave number method developed by Aki and Larner. Amplification characteristics are discussed by comparing the observed data with the theoretical estimates. The theoretical estimates by both methods agree well with the observed results in low frequency range, i.e. as long as incident wavelengths are larger than the dimension of a horizontal discontinuity.

1. Introduction

Reports of earthquake damage have been frequently noted that the damage is sometimes confined to small zones, where local geological configulations have steeply lateral variations. For example, the intense damage at the 1963 Scopie Earthquake is recorded along a belt which is defined by an abrupt change of the thickness of the alluvium (Poceski, 1969).[1] The 1976 Northern Yamanashi Earthquake in Japan concentrates the damage remarkably along the Tsurukawa fault belt, although this fault is away from the source area (Murai, et al., 1977).[2] Furthermore, we can note a lot of similar cases in recent large earthquakes, such as the 1978 Sea-Off-Miyagi Earthquake (Japan) and the 1980 Northern Italy Earthquake. These show it is necessary for the engineer-seismological study to estimate amplification effects of ground motions by lateral interference associated with geological irregularity as well as vertical interference within flat surface layers.

In recect years, several studies have been done on the theoretical or numerical calculations of amplification characteristics of seismic waves due to horizontal irregularities in surface layers (e.g., Hong and Helmberger, 1978;[3] Boore, et al., 1971;[4] Sanchez-Sesma and Esquivel, 1979)[5]. However, only a few observed field data have been reported (e.g., Rogers. A.M., et al., 1979).[6] The first purpose of this study is to estimate directly the amplification effects by observing ground motions in the area having a horizontal discontinuity. The second purpose is to discuss the validity and range of applicability of some theoretical methods by comparing the observed data with the theoretical estimates. Two practical methods are examined to calculate numerically the seismic responses for SH waves in a multilayered medium containing a layer with lateral steep variation of velocity. One is a singular integral equation method developed by Kennett (1973, 1974),[7),8] and the other is a discrete wave number method developed by Aki and Larner (1970).[9]

2. Geological Feature of Observation Sites and Method of Observations

The study area is located at the eastern side of the southern part of Kyoto basin, as shown in the right-lower insert of Fig. 1. There extends a plain to the west of this area which approaches hills to the east. It is reported that the plain part is formed of alluvium and diluvium and the hill part is composed of paleozic strata (Kitsune-

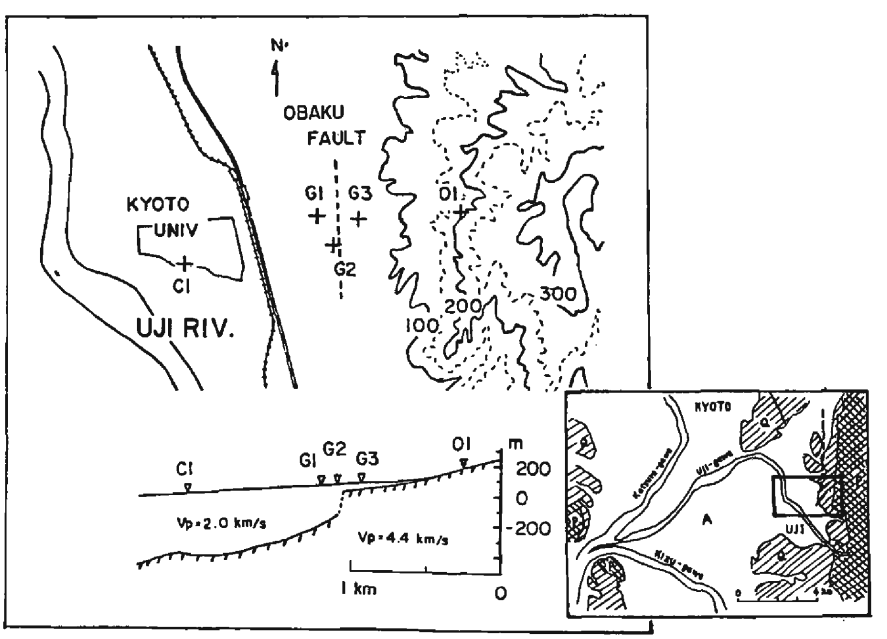

Fig. 1. Topographical map showing the location of the observational points, C1, G1, G2, G3 and O1, and vertical cross section of underground structures.
P: Paleozoic rocks, Q: Terrace deposits of deluvium, A: Alluvial deposits.

zaki, et al., 1971).[10]

The underground structure in this area was first estimated by Kitsunezaki et al. in 1971, as shown in the lower part of **Fig. 1.** They carried out seismic refraction exploration by means of five explosion sources on a long mesuring line of about 12 km, ranging from the middle part of the basin to the eastern edge. In that survey, they found out that the thickness of soil deposits changed abruptly (about 150–200 m) on the eastern side of the basin and the discontinuity was inferred to be located on an extension of the Obaku fault. In order to determine the underground structures in detail near the postulated fault, Kobayashi, et al. (1980)[11] carried out refraction exploration on a short measuring line of about 600 m across the fault by a procedure of a stacking method employing a land-type air gun.

The east-to-west underground profile in the vicinity of the fault is shown in **Fig. 2** obtained by the above two explorations and boring data. The soil deposits are formed of two layers: alluvium and diluvium. The upper layer (alluvium) has a thickness of 10 to 20 m and a P wave velocity less than 1 km/sec. The lower layer has a laterally discontinuous thickness, which is thick on the west side of the fault and thin on the east side. From boring data, there evidently exists the base rock, underlying the soil deposits, at depth of about 50 m on the east side of the fault, i.e. hill side. On the other hand, we find that the depth to the base rock is more than 180 m on the west side, i.e. basin side.

Earthquake ground motions have been observed at 5 points indicated with (+) marks in **Fig. 1.** O1 point, located at about 1 km east to the fault, is on the

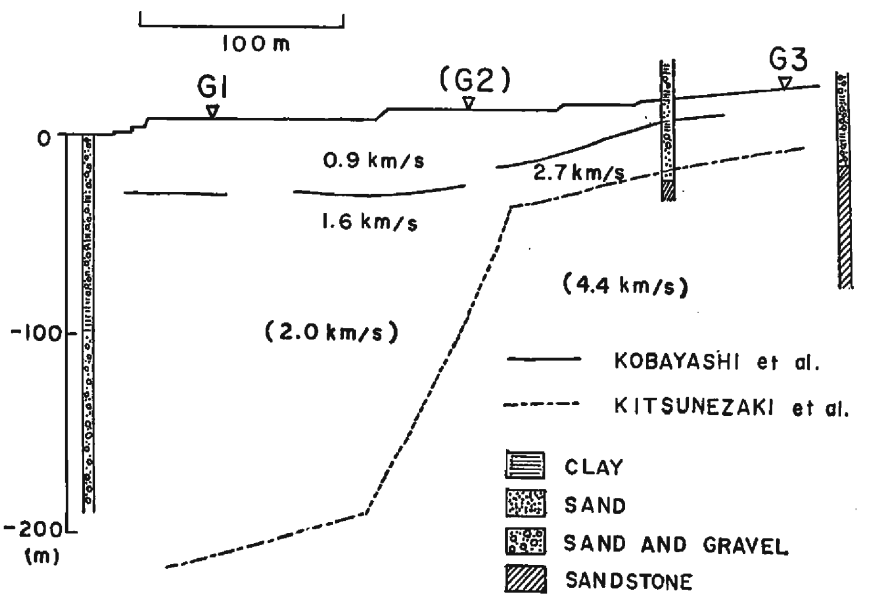

Fig. 2. Comparison between P wave's velocity structures in the vicinity of the Obaku fault determined by Kitsunezaki, et al. (1971) and those by Kobayashi, et al. (1980).

rock outcrop, C1 point, about 1 km west to the fault, is underlain by thick soft layers, and three points, G1, G2, and G3 are set in the immediate vicinity across the fault (each interval is about 300 m).

The sensing instruments are 3-component sets of velocity seismometers having a natural period of 2.0 sec, a sensitivity of 1 volt/kine and a damping ratio of 0.64 to critical at the points except C1, and 3.0 sec, 2 volt/kine, 0.64 at C1. The output singals from each seismometer are recorded in analog form using a magnetic tape recorder, after being amplified 50 to 200 times through DC type amplifiers. The data on magnetic tape are converted to digital form at the sampling interval of 0.005 sec through an A-D converter.

3. Data Analysis and Interpretation

3.1 Spectral Analysis Method

To estimate layer transfer functions associated with surface layers, it is necessary to obtain the spectra of surface ground motions and incident waves from the bed rock to surface layers. To obtain the incident seismic waves, direct observation should be made at the bed rock underground (deeper than 500 m in this study area). In practice, however, it is usually very difficult to carry out such observation. In this study, seismic motions observed on a rock outcrop are regarded as the incident waves at the bed rock, and transfer functions associated with near surface layering are estimated by comparing the motions on the soft grounds with those on the rock outcrop. Effects of the surface topography on seismic motions at this rock site are discussed by Irikura (1980).[12] The azimuthal differences of the surface motions due to surface topographical effects at the rock site are reported to be, at the highest, less than 8 per cent within the frequency range of interest. We consider seismic motions at the rock site can be put into the incident waves as the first approximation.

Some care has to be taken when computing Fourier spectra of the ground motions, because spectral ratios generally have different values dependent on the methods of spectral calculations. Even if Fourier transform can be calculated exactly using, for example, F.F.T. (Fast Fourier Transform) method, Fourier spectra of observed ground motions often show oscillatory character. This oscillatory character of the Fourier amplitude spectra can be understood as the result of the response of the layer to a sequence of discrete wave-arrivals of different types, each characterized by its own incident angle (Murphy et al., 1971).[13] In addition, when making a calculation, truncation effects also cause the oscillatory spectra. To supress the oscillations in the spectral shapes, smoothing of spectra is required, although the physical significance of smoothing is not always clear. Fourier transform without smoothing is not adequet to calculate spectral ratios, because this oscillatory character tends to increase errors in the spectral ratio computation. B.T.M. (Blackman and Tukey Method) is one of the conventional methods of smoothing, but it has a

defect of low resolution for short records because this technique requires the computation of auto-correlation function by using a zero extension of the data. On the other hand, M.E.M (Maximum Entropy Method) is superior in resolution because auto-correlation functions are predicted by using given finite auto-coveriance functions.

An example of comparison between the spectra calculated by F.F.T. and those by M.E.M. is shown in **Fig. 3.** M.E.M. spectra are calculated by auto-covariance functions (A.F. method). The M.E.M. spectra are clearly smooth, just like the appropriate running mean ones of F.F.T. spectra. Application of the M.E.M. to the spectral analysis of seismic signals is discussed in detail by Ouchi and Nagumo (1975).[14] In calculating the spectra by M.E.M. there are two methods of computing the filter coefficients; the A.F. method in which auto-covariance functions are directly calculated, and the Burg method, which is well known as Burg algorithm (Ulrich, 1972).[15] It is reported by Saito (1974)[16] that the Burg method is not suitable for nonstationary minimum phase data of short length. Kishimoto (1980)[17] has examined the two methods by calculating the spectra for input test signals of various kinds, and showed that the A.F. method is usually better than the Burg method. Another significant problem in employing M.E.M. calculation is how large the filter length should be taken. Akaike's criterion, F.P.E. (Final Prediction Error), seems to be very useful in determining filter length, however, it does not always give reasonable results. In general, it is known that best filter length is somewhat larger than that given by F.P.E. criterion, particularly for periodic signals.

Considering these facts, we calculated the spectra of observed seismograms using the A.F. method for data length, 10.24 sec, and filter length, 1.5 sec, in this

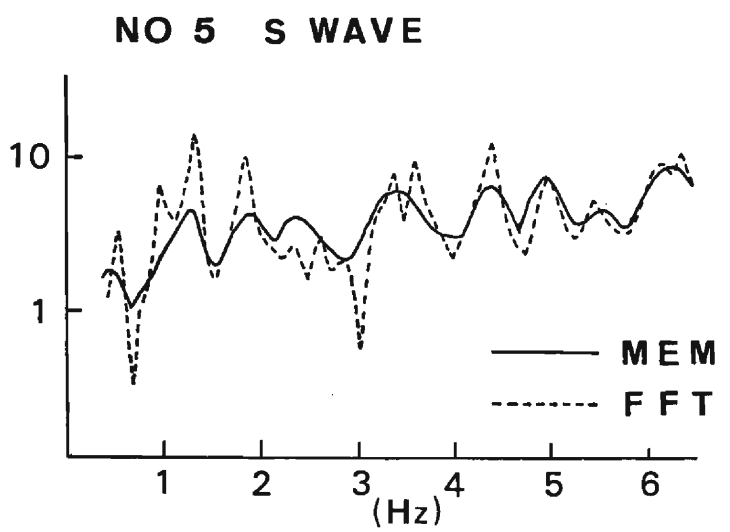

Fig. 3. Comparison between spectral ratios calculated by F.F.T. and those by M.E.M.

study.

3.2. Analysis of Data from Deep Earthquakes

An analyzed example of ground motions from a deep earthquake is shown in **Fig. 4** and **Fig. 5.** The wave-form and the Fourier spectrum of S wave motions at each point are compared, and spectral ratios of the ground motions at 4 points (G1, G2, G3, and C1, underlain by soft surface layers) to the rock motions at O1 point are computed to estimate the amplification effects due to the underground structures.

In the case of a deep earthquake from short distance, the seismic waves approach these points with nearly vertical incidence. The three spectral ratios of NS component, G1/O1, G2/O1, and G3/O1 have a significantly common peak around 1.5 Hz. Those of EW component do not always have such significant common-peaks. The ratio, C1/O1 shows a different tendency, having two significant peaks around 0.5 Hz and 1.5 Hz. Another example of spectra and spectral ratios derived from another deep earthquake are shown in **Fig. 6.**

It is very difficult to separate SH wave from SV wave and to identify the same phases between the two sites. In this study, the spectral ratios of $\sqrt{Es}$, given by $\sqrt{NS^2+EW^2}$, are computed to estimate the ground responses due to SH waves as a practical method. When the S wave's velocities of surface layers are remarkably lower than those of bed rock, the ground responses due to SV waves are like those due to SH waves. Thus, $\sqrt{Es}$ may be considered to approximate the SH wave

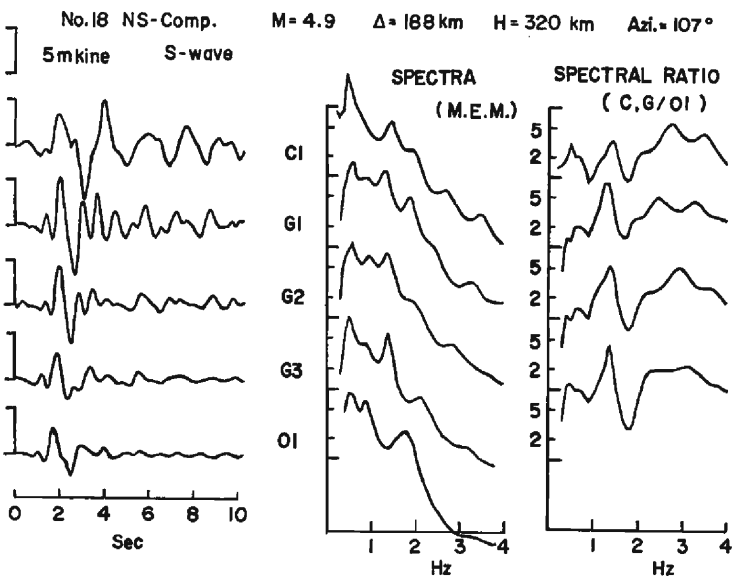

Fig. 4. Waveforms and Fourier spectra of NS-component of S wave's ground motions from a deep earthquake and spectral ratios, C1/O1, G1/O1, G2/O1 and G3/O1.

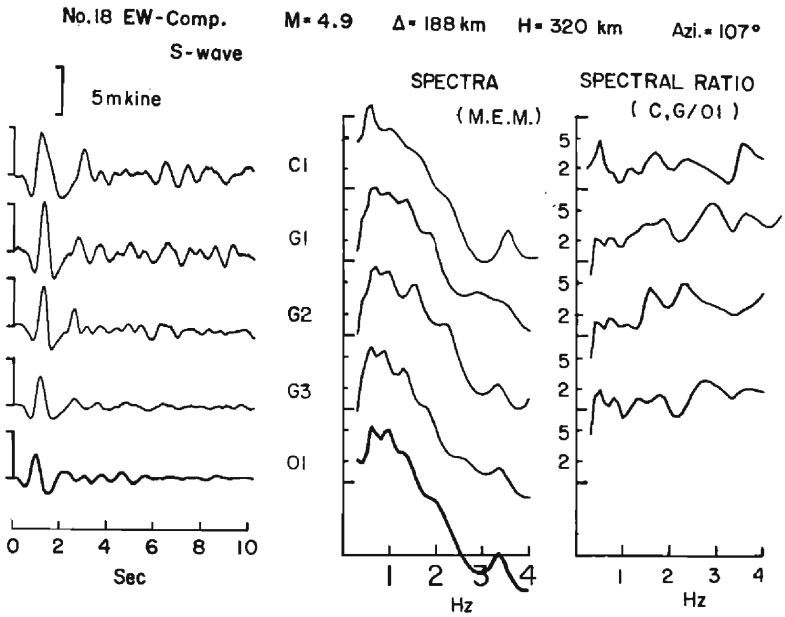

Fig. 5. Waveforms and Fourier spectra for EW-component.

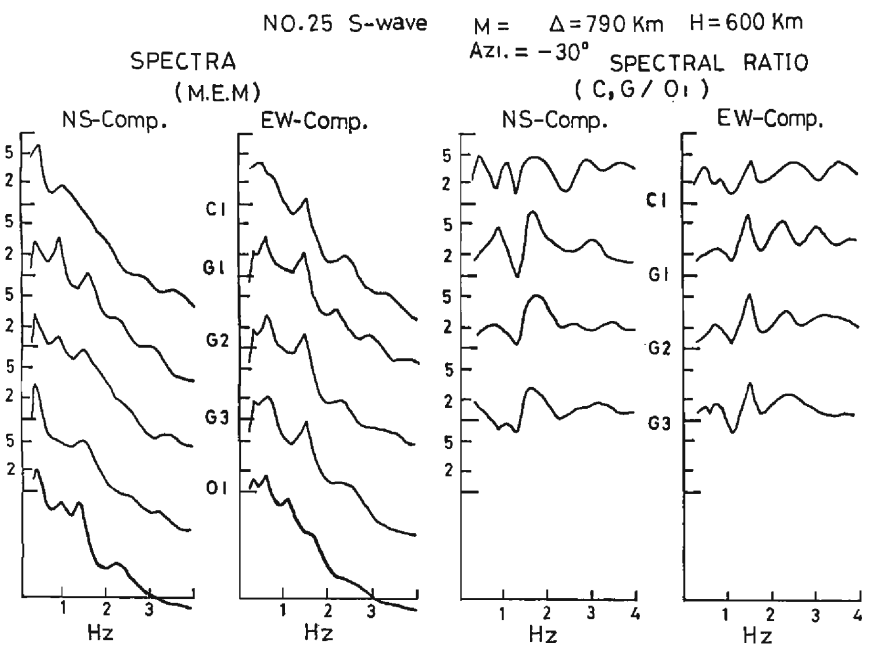

Fig. 6. Fourier spectra of S wave's ground motions (NS, EW component) from a deep earthquake and spectral ratios, C1/O1, G1/O1, G2/O1 and G3/O1.

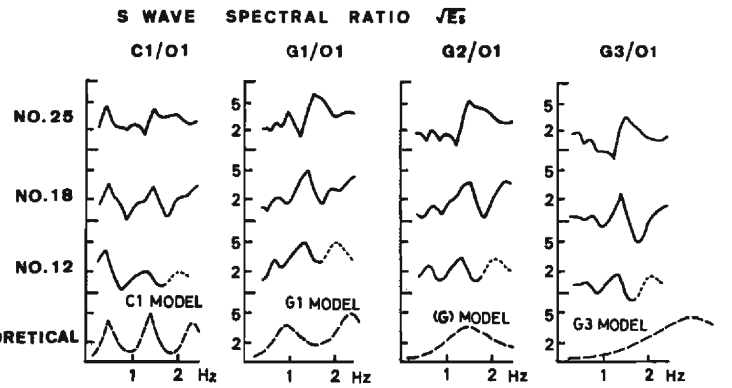

Fig. 7. The comparison of the spectral ratio at each point with the theoretical response calculated by the conventional matrix method.

Table 1. Layered models at the ground sites.

LAYERED MODEL
[S VELOCITY (m/s): DENSITY (g/cm³): THICKNESS (m)]

C1			G1			(G)			G3		
250	1.7	3	250	1.7	5	250	1.7	5	250	1.7	5
440	1.8	12	500	1.9	50	500	1.9	20	500	1.9	20
320	1.8	6	750	2.1	150	750	2.1	100	750	2.1	20
580	1.9	11	1400	2.5		2400	2.5		2400	2.5	
460	1.9	8									
580	2.0	80									
750	2.1	250									
2400	2.5										

ground-responses in this area.

In **Fig. 7,** the spectral ratios of $\sqrt{Es}$ from three deep earthquakes are compared with theoretical responses due to the underground structures immediately beneath the site, using a conventional matrix method with flat layers assumption. Each layered model is determined from seismic prospecting and boring data. The C1 model response is in good agreement with the observed results as shown in **Table 1.** Two predominant peaks around 0.5 Hz and 1.5 Hz correspond to the fundamental and the first higher mode resonant-frequencies respectively in the thick soft layers. This indicates that amplification characteristics at C1, about 1 km away from the fault, are not so significantly affected by the fault structure in the deep earthquake cases. On the other hand, the theoretical responses of G1 and G3 models assuming flat layers are not consistent with observed ones. The spectral ratios at the three points, G1, G2 and G3, have commonly predominant peaks whose frequencies are almost the same and amplitudes are different from one another, as shown in **Fig. 7.** (G) model is assumed as the structures with averaged properties of those on both sides of the fault. The predominant frequencies of the spectral ratios, G1/O1, G2/O1, and

G3/O1 tend to agree with that of response of (G) model, assumed as an average, rather than those of G1 and G3 model, assumed by considering structures directly beneath each point. Naturally, the amplitude variation of the spectral ratios can not be explained by the (G) model.

The amplitudes of the common peaks are considered to be different depending on the site conditions of the three points. That is, amplification factors corresponding to the peak amplitudes of the ratios increase with the increasing thickness of the soft layers directly beneath each point. The frequencies of the common peaks vary slightly (1.4 Hz–1.6 Hz), in detail, for the three earthquakes. The slight difference between these peak frequencies may be caused by the difference of the azimuth and the angle of incidence of seismic waves.

3.3 Analysis of Data from Shallow Earthquakes

In **Fig. 8**, analyzed examples of ground motions from shallow earthquakes are shown. The seismic waves are considered to approach these sites at oblique incidence. The left figures show the cases of the waves arriving from the west, that

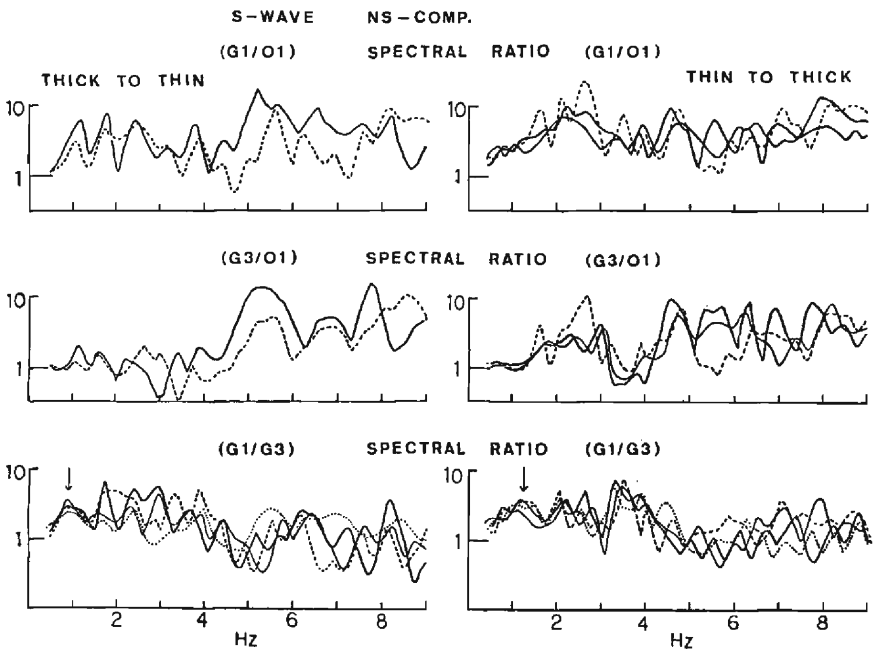

NO. 5	M=3.1	Δ=82KM	AZI.=−165°	NO.11	M=3.9	Δ=152KM	AZI.=57
19	2.7	87	−139°	17	3.5	184	57
7	3.6	89	−13°	2	4.5	142	48
20	4.6	50	−155°	6	3.7	105	50

Fig. 8. The spectral ratios of seismic waves, G1/01, G3/01 and G1/G3, from shallow earthquakes. Left is the case of seismic waves arriving from west, i.e. thick to thin layers and right is the case, from east, i.e. thin to thick layers. M; magnitude, △; epicentral distance, AZI; azimuth of the epicenters from the site measured clockwise from the north.

is propagating from thick soft layers to thin ones, and the right figures show the cases from the opposite direction. The spectral ratios, G1/O1 have significantly larger factors than do the ratios, G3/O1, in the lower frequency range (lower than 5 Hz in **Fig. 8**), although they have factors of the same order in the higher frequency range. This is caused by lateral variations of the soft layer thickness. Since the higher frequency components of the amplitudes are controlled by the near-surface structures which are over the layer containing the fault, they are not strongly affected by the lateral variations of the layer thickness.

The peak frequencies of the spectral ratios have a tendency to shift to lower frequencies in the case of incident waves from thick to thin layers than those in the case of thin to thick. The lowest peak frequency of G1/O1 tends to be around 1 Hz in the former case, and higher than 1.5 Hz in the latter case. This tendency suggests that the spectral characteristics of amplifications are affected by the underground structures including the adjacent areas in propgation of seismic waves, when seismic waves are obliquely incident.

4. Seismic Responses for Incident SH Waves in a Multilayered Medium Having a Lateral Discontinuity

The assumption of laterally uniform underground structures can not be always compatible with the tendencies of amplification characteristics mentioned above, deduced from the observed data. It is necessary to estimate the effect of the ground structures with laterally steep variations on seismic motions.

Seismic responses for incident SH waves are calculated by Kennett (1973, 1974) in a medium containing a layer in which there is a horizontal discontinuity in elastic parameters. In his method, motion-stress vector $\boldsymbol{B}$ is expressed as the following singular integral equations.

$$\boldsymbol{B}(k,z,w) = \mathrm{P}(k,z,z_0)\boldsymbol{B}(k,z_0,w)+\mathrm{S}(k)$$

$$\mathrm{S}(k) = \int_{z_0}^{z} \mathrm{P}(k,z,y)\{\mathrm{a}(k)\int_{-\infty}^{\infty} \boldsymbol{B}^0(x,y,w)\,\mathrm{sgn}(x)\,\mathrm{e}^{-ikx}dx+\mathrm{c}(k)\,(\boldsymbol{J}_+^0+\boldsymbol{J}_-^0)\}dy$$

$$\boldsymbol{B}^0 = \boldsymbol{B}_-^0\mathrm{H}_-(x)+\boldsymbol{B}_+^0\mathrm{H}_+(x) \qquad \mathrm{H}_+(x) = \begin{cases} 0 & x<0 \\ 1 & x\geq 0 \end{cases} \qquad \mathrm{H}_-(x) = \begin{cases} 1 & x<0 \\ 0 & x\geq 0 \end{cases}$$

In the notation above, P is a propagator matrix corresponding to the average media on both sides of the fault, $\mathrm{a}(k)$ and $\mathrm{c}(k)$ are matrices dependent on the elastic parameter contrasts across the fault plane. $\boldsymbol{B}_\pm^0$ are local motion-stress vectors on either side of the fault, and $\boldsymbol{J}_\pm^0$ are motion-stress vectors at the fault plane. Seismic waves through the fault layer are expressed by the equation with sum of two terms. The first term corresponds to the effect of the propagation of incident wave through the media with averaged properties on both sides of the fault. The second represents diffracted waves corresponding to the effect of the sources introduced to allow for the effect of the lateral discontinuity. Kennett calculated the responses only for a

simple model, i.e. infinite medium containing a layer in which there is a horizontal discontinuity. We evaluated the above equation considering the effect of adding a free surface to the medium.

Seismic responses for incident SH waves in layered media having a laterally irregular interface are also calculated by Aki and Larner (1970). They developed a practical method based on a discrete wave number representation of elastic wave fields in which scattered wave field is described as a superposition of plane waves. The discretization results from a periodicity assumption in the discription of the medium, so that integral equations of boundary conditions in wave number domain reduce to infinite-sum equations.

5. Computed Results and Discussion

5.1 Computation for Vertical Incidence

Theoretical responses are shown in **Fig. 9**, calculated by these two methods

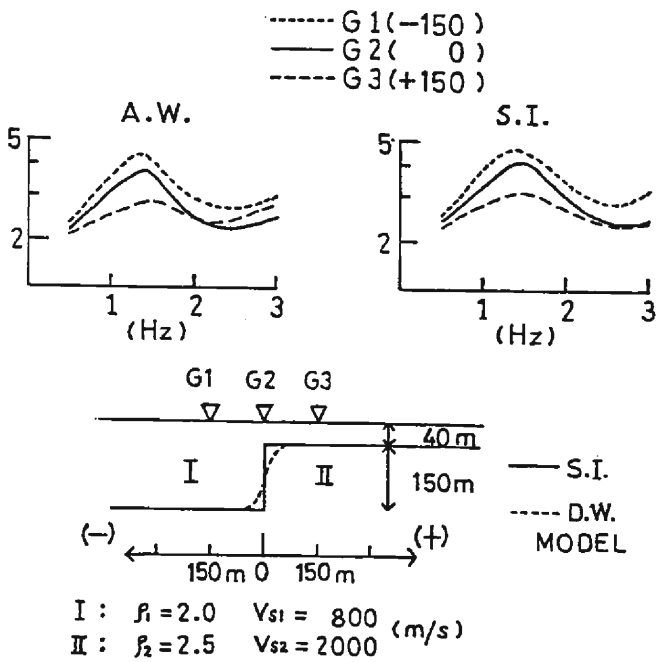

Fig. 9. Upper part; Spectral amplitudes of the theoretical responses at the three points, G1, G2 and G3, for vertically indicent SH waves. Left shows the responses calculated by D.W., Discrete Wave number method (Aki and Larner, 1970). Right shows those by S.I., Singular Integral equation method (Kennett, 1973, 74).
Lower part: Assumed S-wave's velocity-structure models and the location of G1, G2 and G3. D.W. model is slightly different form S.I. model.

for vertically incident SH waves which correspond to the wave-field model of the incidence of the seismic waves from a deep earthquake. The underground structure model is simplified as shown in the lower part of **Fig. 9.**

If the maximum slope of the irregular interface is fairly large, the intrinsic error becomes larger beyond an acceptable level in the discrete wave number method. On the contrary, the singular integral equation method calculates the responses less acurately as the slope of the interface at the horizontal discontinuity becomes smaller. Thus, the assumed velocity structure model in these two methods is restricted to be a little different from each other, as shown in Fig. 9, to keep the error less than a tolerable level. The errors of numerical calculations are discussed later in this section.

Comparing **Fig. 6** with **Fig. 9**, we find that the calculated amplifications by both methods and the observed values derived from the deep earthquakes are in good agreement. That is, the observed common-peaks around 1.5 Hz at the three points across the fault are apparent in the calculated responses. Besides, other observed results are obtained which show that amplification factors at the predominant frequencies increase with the increasing thickness of the soft layer directly beneath each point.

To estimate the spatial distribution of amplification factors, theoretical amplification factors at the frequency of 1.0 Hz are plotted versus horizontal distance from the fault in **Fig. 10.** This frequency approximately corresponds to the resonant frequency of the fundamental mode on the side of the thicker surface layer due to vertical constructive interferences. Amplification factors become gradually lar-

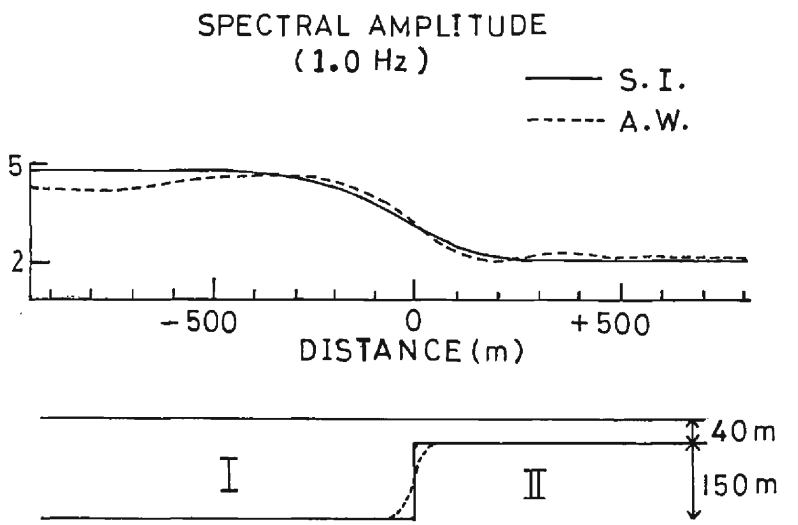

Fig. 10. Spatial distributions of response amplutides at 1.0 Hz for vertically incident SH waves. The broken line is the response calculated by the discrete wave number method. The solid line is the response by singular integral equation method. The assumed S wave's velocity-structures are the same as in Fig. 9.

ger over a distance of about 400 m (half wavelength in surface layer), as the site moves from the thin to thick layer. This example shows that the resonance condition at each site is affected by underground structures including adjacent areas.

5.2 Computation for Oblique Incidence

Theoretical responses for obliquely incident SH waves from different directions are compared in **Fig. 11**, calculated by the discrete wave number method. Seismic waves from shallow earthquakes are considered to approach the fault at oblique incidence. In the left of this figure, the theoretical curves correspond to the responses for incident waves approaching from the thick to thin layer, and the right figure shows them for incident waves from the opposite direction.

There is a significant difference between these two responses for the opposite seismic arrivals from each other. The peak frequencies of the theoretical amplifications have a tendency to shift to lower frequencies in the case of incidence from the thick to thin layer than in the case from the thin to thick layer. That is, peak frequencies at G1 in the former case are around 1.1 Hz, but in the latter case, around 1.5 Hz. Similarly, the lowest peak frequencies at G3 are around 1.5 Hz in the former case, but higher than 2.5 Hz in the latter case. This tendency of the theoretical responses resembles that of observed spectral ratios, G1/O1 and G3/O1.

The dependence of amplification characteristics on the direction of incident waves seems to be more evident in the observed values than in the theoretical responses. This is partly because of oversimplification of the assumed underground-structure

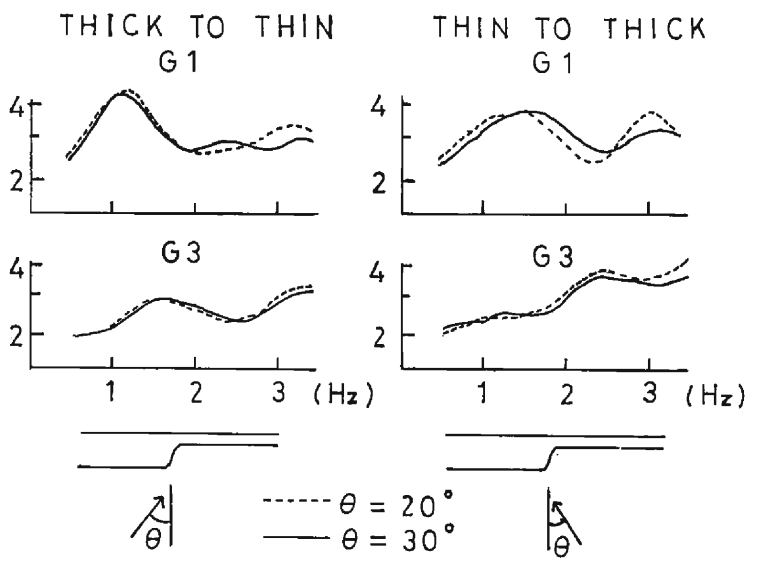

Fig. 11. The variations of amplitude characteristics at G1 and G3 with the directions of the seismic arrivals, calculated by discrete wave number method. Left is the case of incident waves arriving from thick to thin layers. Right is from thin to thick layers.

model in the theoretical computation. The P-wave refraction survey in this area shows that the thickness of surface layers increases gradually toward the west, from the fault to the center of the basin. The observed amplification characteristics in the vicinity of the fault may be affected by the dipping underground structures. But datailed comparison between the observed values and the theoretical computations is difficult at present because of scarcity of observed ground-motion data and the information concerning S wave velocity structures.

5.3 Errors of Numerical Calculations.

In the Kennett method, computational errors become larger as the discontinuity length increases, or as the incident wave length and slope of the interface becomes smaller. The range of applicability of this method is defined by the following condition. (Kennett 1974)

$$\frac{\omega H \eta}{\pi \beta_{\min}} \sec \theta \ll 1$$

where H is the thickness of the discontinuous layer, η is the reflection coefficient, and θ is the slope of interface. For the velocity structure model in this study area, incident wave frequencies are restricted to be no higher than 4 Hz.

The response in time domain for a low-frequency incident-pulse shows the result of overlapping of transmitted and reflected waves from discontinuous layer and diffracted waves generating from the discontinuity. In this case, the diffracted waves are hardly visible separately from other phases. It is necessary to calculate the response for a high frequency pulse, to examine the accuracy of diffracted wave calculation, which Kennett (1974) actually calculated.

We calculated the following response models; the response of the structure having a thin discontinuous layer (10 m) for vertically incident high-frequency pulse (20 Hz). The computation model used here is extended to the half space model, while Kennett dealt with only the infinite model.

Response wave forms are shown in **Fig. 12** at various distances from the discontinuity. Diffracted waves arising from the fault plane, as well as transmitted waves and reflected waves are clearly seen in this figure. Diffracted waves show a radiation pattern due to a line of double couples along the fault, and attenuate with increasing distance from the fault. The amplitude just at the end of the reflecting horizon of the fault layer should be half of the full reflected wave, after Trorey (1970).[19] In this computation, the ratio is in quite good agreement with his simple theory of seismic diffraction. But there are small noises in the region where no reflection is expected. This indicates the degree of error in this calculation method. Amplitudes of the computational noises are about 5 per cent of the incident wave amplitude.

In the Aki and Larner method, the intrinsic error, known as "Rayleigh anzats error," becomes larger as the discontinuity length and maximum slope of the interface increases or as the incident wave length becomes smaller. The discrepancy of

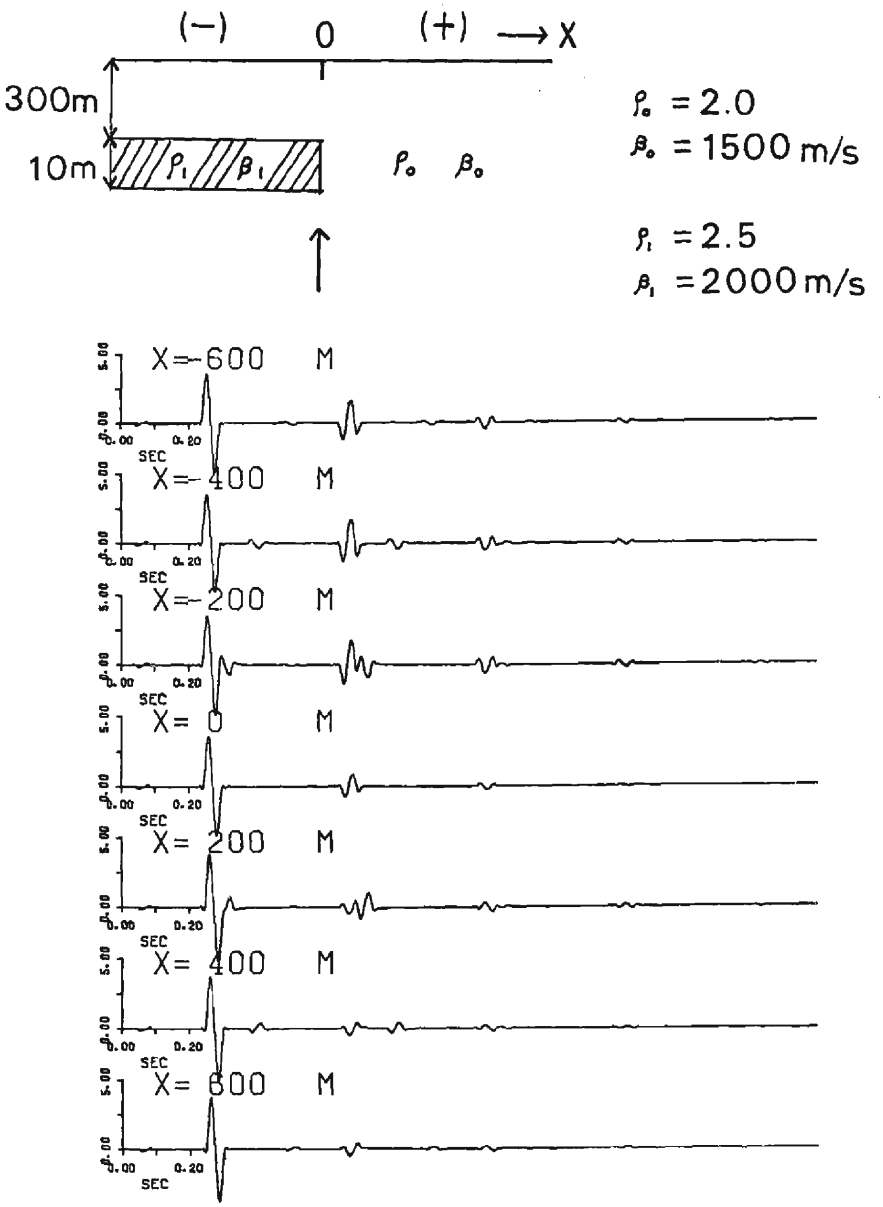

Fig. 12. Displacement traces for a normally incident plane pulse showing reflected, transmitted and diffracted waves from a 10 m thick truncated layer, calculated for varing horizontal separations X from the fault (in meters) on a free surface.

displacement and stress at the interface becomes larger, as the slope of the discontinuity is steeper. As a measure of accuracy of this calculation, Aki and Larner defined relative root-mean-square (rms) error as the following:

$$(\mathrm{RMSE})^2 = \frac{\sum_{j=1}^{M}\left(\left|\frac{\hat{u}_j\omega}{\beta_1}\right|^2+\left|\frac{\hat{\tau}_j}{\mu_1}\right|^2\right)}{\sum_{j=1}^{M}\left(\left|\frac{u_{1Nj}\omega}{\beta_1}\right|\left|\frac{u_{2Nj}\omega}{\beta_1}\right|+\left|\frac{\tau_{1Nj}}{\mu_1}\right|\left|\frac{\tau_{2Nj}}{\mu_1}\right|\right)}$$

where $\hat{u}_j$ and $\hat{\tau}_j$ are the displacement and stress discrepancy (residuals) respectively, at position j along the interface; u_{1Nj} and u_{2Nj} are computed values of displacement at position j along the intertace in the layer and half-space, and τ_{1Nj} and τ_{2Nj} are the computed stresses at those positions. In this study model, (rms) errors are within 15 per cent in the frequency band lower than 3 Hz. An example of (rms) errors for incident waves of various frequencies is shown in **Fig. 13**. Effects of frequency characteristics of (rms) error on surface motion amplitudes are considered to be less than these values in spatial average. The influence of the amplitude distribution due to the localized errors along the interface will be discussed in a later paper.

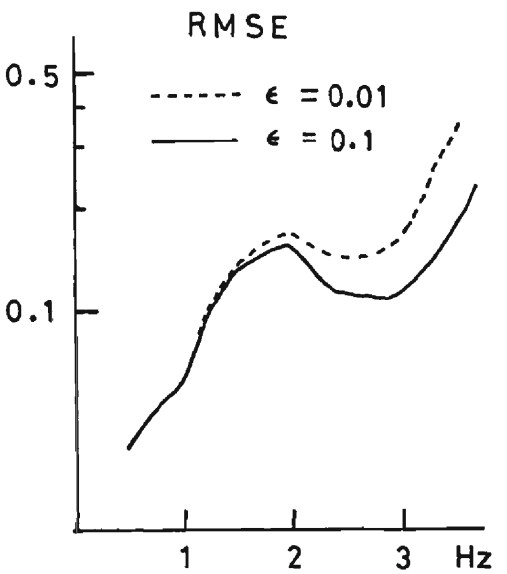

Fig. 13. Root-mean-square errors for incident waves of various frequencies in the numerical calculation by the discrete wave number method. ϵ is the ratio of the imaginary to real parts of frequency.

6. Conclusion

The observed amplification effects due to soft surface layers on the ground sites have the following features.

1) In the case of seismic waves from deep earahquakes which are nearly vertically incident to the area, amplification characteristics at the 3-points across the fault

have remarkable common-peaks around 1.5 Hz.

2) However, amplification factors at this common peak frequencies are larger with the increasing thickness of soft surface layers immediately beneath each point.

3) In the case of seismic waves from shallow earthquakes which are obliquely incident, the peak frequencies of the amplifications vary with the directions of seismic arrivals, shifting to lower frequencies for propagation of the thick to thin surface layers than those for propagation of the thin to thick layers.

These tendencies of the observed amplifications are approximately explained by the theoretical responses calculated by the singular integral equation method and the discrete wave number method. Comparing the observed values with the theoretical ones, we find they are in good agreement in the low frequency range, which is lower than about twice the fundamental resonant-frequency of the thicker layer.

These results indicate that in the area having steep horizontal discontinuity, amplification characteristics at a given site are strongly influenced by the structures involving adjacent areas in propagation of seismic waves. Spectral characteristics of amplifications across the discontinuity are similar to each other, as long as the incident wavelengths are larger than the dimension of horizontal discontinuity. However, amplification factors at the predominant peaks are different from each other, growing larger with the increasing thickness of surface layers.

Acknowledgements

We wish to express our appreciation to Prof. Soji Yoshikawa for many suggestions. We also thank Prof. Michiyasu Shima for his encouragement in carrying out this work.

Our thanks are also due to Associate Prof. Yoshimasa Kobayashi for his helpful advice and Mr. Masanori Horike, Mr. Fumio Amaike, and Mr. Kiyoyuki Kishimoto for their valuable discussions. We are especially grateful to Mr. Masao Nishi for his co-operation in the observation and Mrs. Kazue Kutsuki for arranging the data.

The data processing was run on a FACOM M-140 at the Information Data Processing Center for Disaster Prevention Reseach, of Disaster Prevention Reseach Institute of Kyoto University and the numerical computations were run on a FACOM M-200 at the Data Processing Center of Kyoto University.

References

1) Poceski A.: The Ground Effect of the Scopie July 26 1963 Earthquake, Bull. Seism. Soc. Am., Vol. 59, 1969, pp. 1–22.

2) Murai, I., N. Tsunoda and Y. Tsujimura: Inquiry Survey of Intensity Distributions on the Northern-Yamanashi Earthquake in 1976, Proc. 14 the Japan Natio. Cong. Natur. Disast. Sci., 1977, PP. 387–388 (in Japanese).

3) Hong, T.L. and D.V. Helmberger: Glorified Optics and Wave Propagation in Nonplaner Structure, Bull. Seism. Soc. Am. 68, 1978, pp. 1313–1330.
4) Boore, D.M., K.L. Larner, and K. Aki,: Comparison of Two Independent Methods for the Solution of Wave-scattering Problems: Response of a Sedimentary Basin to Vertically Incident SH-waves, J. Geophys. Res., 76, 1971, pp. 558–569.
5) Sanchez-Sesma, F., and J. Esquivel: Ground Motion on Alluvial Valleys under Incident Plane SH Waves, Bull. Seism. Soc. Am. 69, 1979, pp, 1107–1120.
6) Rogers, A.M., J.C. Tinsley, W.W. Hays and K.W. King.: Evaluation of the Relation Between Near-surface Geological Units and Ground Response in the Vicinity of Long Beach California, Bull. Seism. Soc. Am. 69, 1979, pp. 1603–1622.
7) Kennett, B.L.N.: The Interaction of Seismic Waves with Horizontal Velocity Contrasts, Geophys. J.R. astr. Soc., 33, 1973, pp. 431–450.
8) Kennett, B.L.N.: The Interaction of Seismic Waves with Horizontal Velocity Contrasts-II. Diffraction Effects for SH Wave Pulses, Geophys. J.R. astr. Soc., 37, 1974, pp. 9–22.
9) Aki, K., and K.L. Larner,: Surface Motion of a Layered Medium Having an Irregular Interface due to Incident Plane SH Waves, J. Geophys. Res., 75, 1970, pp. 933–954.
10) Kitsunezaki, C., N. Goto and Y.T. Iwasaki.: Underground Structure of the Southern Part of the Kyoto Basin Obtained from Seismic Exploration and Some Related Problems of Earthquake Engineering, Annuals Disast. Prev. Res. Inst., Vol. 14A, 1971, pp. 203–207 (in Japanese).
11) Kobayashi, Y., K. Irikura, M. Masanori, F. Amaike, K. Kishimoto and S. Kasuga: Seismic Exploration of the Obaku Fault, Annuals Disast. Prev. Res. Inst., Vol. 23 B-1, 1980, pp. 95–106 (in Japanese).
12) Irikura, K.: Earthquake Ground Motions Influenced by Irregularities of Sub-Surface Topography, Proc. 7th. World Conf. on Earthq. Eng., Vol. 2, 1980, pp. 175-182.
13) Murphy, J.R., A.H. Davis and N.L. Weaver: Amplification of Seismic Body Waves by Low-Velocity Surface Layers, Bull Seism. Soc. Am., Vol. 61, No. 1, 1971, pp. 109–145.
14) Ouchi, T. and S. Nagumo: On the Application of the Maximum Entropy Method to the Spectral Analysis of Seismic Signals, Bull. Earthq. Res. Inst., Vol. 50, 1975, pp. 359–384.
15) Saito, M.: Possible Instability in the Burg Maximum Engropy Method, J. Phys. Earth., Vol. 26, 1978, pp. 123–128.
16) Olrych, T.J.: Maximum Entropy Power Spectrum of Truncated Sinsusoids, J. Geophys. Res., Vol. 77, 1972, pp. 1396-1400.
17) Kishimoto, K.: In Situ Mesurament of Love Wave Attenuation in Soil Layers and the Estimation of Qs-Structure, Zisin, Vol. 35, No. 1, 1982, pp. 1–18. (in Japanese).
18) Akaike, H.: Fitting Autoregressive Models for Prediction, Ann. Inst. Stat. Math., Vol. 21, 1969, pp. 261–265.
19) Trorey, A.W.: A Simple Theorey for Seismic Diffractions, Geophysics, Vol. 35, No. 5, 1970, pp. 762-784.